Differential role of cytosolic Hsp70s in longevity assurance and protein quality control

Rebecca Andersson[1], Anna Maria Eisele-Bürger[1,2,#a¶], Sarah Hanzén[1,#b¶], Katarina Vielfort[1,#c¶], David Öling[2,#d¶], Frederik Eisele[1,2,#a], Gustav Johansson[2,#e], Tobias Gustafsson[2,#f], Kristian Kvint[2,#g], Thomas Nyström[1,2,#a*]

[1] Department of microbiology and immunology, Institute of Biomedicine, Sahlgrenska Academy, University of Gothenburg, 403 50 Gothenburg, Sweden

[2] Department of chemistry and molecular biology, Faculty of Science, University of Gothenburg, 403 50 Gothenburg, Sweden

[#a] Department of Microbiology and Immunology, Institute of Biomedicine, Sahlgrenska Academy, University of Gothenburg, 403 50 Gothenburg, Sweden

[#b] Cochlear Nordic AB, 435 33 Mölnlycke, Sweden

[#c] Department of Molecular Biology, Umeå University, 901 87 Umeå, Sweden

[#d] Discovery Biology, Discovery Sciences, Innovative Medicines and Early Development Biotech Unit, AstraZeneca R&D, 431 50 Mölndal, Sweden

[#e] Department of Pathology and Genetics, Institute of Biomedicine, Sahlgrenska Academy, University of Gothenburg, 403 50 Gothenburg, Sweden

[#f] Department of Biochemistry and Molecular Pharmacology, University of Massachusetts Medical School, Worcester, MA 01605, USA

[#g] Department of Infectious Diseases, Institute of Biomedicine, Sahlgrenska Academy, University of Gothenburg, 403 50 Gothenburg, Sweden

*: Corresponding author
E-mail: thomas.nystrom@cmb.gu.se

¶: These authors contributed equally

ABSTRACT

70 kDa heat shock proteins (Hsp70) are essential chaperones of the protein quality control network; vital for cellular fitness and longevity. The four cytosolic Hsp70's in yeast, Ssa1-4, are thought to be functionally redundant but the absence of Ssa1 and Ssa2 causes a severe reduction in cellular reproduction and accelerates replicative aging. In our efforts to identify which Hsp70 activities are most important for longevity assurance, we systematically investigated the capacity of Ssa4 to carry out the different activities performed by Ssa1/2 by overproducing Ssa4 in cells lacking these Hsp70 chaperones. We found that Ssa4, when overproduced in cells lacking Ssa1/2, rescued growth, mitigated aggregate formation, restored spatial deposition of aggregates into protein inclusions, and promoted protein degradation. In contrast, Ssa4 overproduction in the Hsp70 deficient cells failed to restore the recruitment of the disaggregase Hsp104 to misfolded/aggregated proteins, to fully restore clearance of protein aggregates, and to bring back the formation of the nucleolus-associated aggregation compartment. Exchanging the nucleotide-binding domain of Ssa4 with that of Ssa1 suppressed this 'defect' of Ssa4. Interestingly, Ssa4 overproduction extended the short lifespan of *ssa1*Δ *ssa2*Δ mutant cells to a lifespan comparable to, or even longer than, wild type cells, demonstrating that Hsp104-dependent aggregate clearance is not a prerequisite for longevity assurance in yeast.

AUTHOR SUMMARY

All organisms have proteins that network together to stabilize and protect the cell throughout its lifetime. One of these types of proteins are the Hsp70s (heat shock protein 70). Hsp70 proteins take part in folding other proteins to their functional form, untangling proteins from aggregates, organize aggregates inside the cell and ensure that damaged proteins are destroyed. In this study, we investigated three closely related Hsp70 proteins in yeast; Ssa1, 2 and 4, in an effort to describe the functional difference of Ssa4 compared to Ssa1 and 2 and to answer the question: What types of cellular stress protection are necessary to reach a

53 normal lifespan? We show that Ssa4 can perform many of the same tasks as Ssa1 and 2, but
54 Ssa4 doesn't interact in the same manner as Ssa1 and 2 with other types of proteins. This
55 leads to a delay in removing protein aggregates created after heat stress. Ssa4 also cannot
56 ensure that misfolded proteins aggregate correctly inside the nucleus of the cell. However, this
57 turns out not to be necessary for yeast cells to achieve a full lifespan, which shows us that as
58 long as cells can prevent aggregates from forming in the first place, they can reach a full
59 lifespan.

60 **INTRODUCTION**

61 A major task of cellular Protein Quality Control (PQC) is to prevent protein misfolding and
62 unspecific protein aggregation. Molecular chaperones are central components of such PQC
63 and the heat shock protein 70 (Hsp70) chaperones are among the most conserved members
64 of the PQC system. Originally identified in *Drosophila,* Hsp70 homologs have been found in
65 almost all organisms studied (1). Yeast has 14 genes encoding Hsp70 chaperones; nine
66 cytosolic and five organelle/compartment-specific. These Hsp70s aid in essential
67 housekeeping functions, including *de novo* protein folding, protein translocation, and protein
68 degradation (2).

69 The general structural domains of Hsp70 chaperones include a 44 kDa amino-terminal ATPase
70 domain (NBD), an 18 kDa substrate binding domain (SBD), and a 10 kDa C-terminal domain
71 (CTD) which contributes to substrate binding by establishing a lid-like structure over the
72 substrate binding cavity (3-6). Protein refolding by Hsp70s is stimulated by co-chaperones
73 from the Hsp40 and the Hsp110 subfamilies of chaperones (7, 8). Additionally, Hsp70s have
74 a role in clearance of protein aggregates by recruiting members of the Hsp100 family (Hsp104
75 in yeast) to aggregates, as well as aiding Hsp100 proteins in the disaggregation process (9,
76 10).

77 The Stress Seventy sub-family A (SSA) represents the major cytosolic Hsp70 family in yeast
78 and consists of four members: Ssa1-4. Ssa1 and Ssa2 are 97% identical and are both

79 constitutively expressed, while the inducible Ssa3 and Ssa4 are 87% identical to each other
80 and 80% identical to Ssa1/2 (11). The four Ssa isoforms display different spatial/temporal
81 expression patterns but have been thought to be functionally redundant. This notion is
82 supported by the fact that growth can be sustained with the presence of either one of the Ssa
83 isoforms (1). However, there appear to be some functional differences between the isoforms.
84 For example, overproduction of either Ssa3 or Ssa4 as the sole cytosolic Ssa results in
85 increased thermotolerance upon a lethal heat shock, while overproduction of Ssa1 or Ssa2
86 does not, even though Ssa1 has the most efficient refolding activity of the four isoforms *in vitro*
87 (11, 12). In addition, while Ssa1 modulates prion formation of both *URE3* and *PSI*$^{+}$, Ssa2 does
88 not (11, 13).

89 Removal of Ssa1 and Ssa2 results in a markedly increased expression of *SSA4* but not *SSA3*
90 (14), yet this strain suffers from increased sensitivity to heat, defects in several protein quality
91 control activities, and accelerated aging (9, 10, 15, 16). Obviously, the enhanced production
92 of Ssa4 cannot fully compensate for the lack of Ssa1 and Ssa2, which suggest that the
93 increased levels of Ssa4 in cells lacking Ssa1/2 are not high enough to fully restore total Ssa
94 levels to those of the wild type cells (as shown in Oling et al., 2014). Another possibility is that
95 Ssa4 cannot carry out some key functions performed by Ssa1 and/or Ssa2. In this work, we
96 approached these possibilities by increasing Ssa4 levels further using a strong constitutive
97 promoter. We found that increased levels of Ssa4 could compensate for the lack of Ssa1 and
98 Ssa2 in almost all PQC processes except the formation of aggregates around the nucleolus
99 and Hsp104-dependent disaggregation, the latter of which was linked to a failure of the
100 nucleotide-binding domain of Ssa4 to recruit Hsp104 to aggregates. The differential role of the
101 Ssa proteins in preventing aggregate formation and aggregate clearance made it possible for
102 us to distinguish which of these processes are most important for longevity assurance.
103

104 **RESULTS**

105 **Ssa4 overproduction suppresses heat sensitivity and counteracts formation of protein**
106 **aggregates in cells lacking both Ssa1 and Ssa2**

107 As previously reported, cells lacking both Ssa1 and Ssa2 display reduced thermotolerance
108 (fig. 1A). By using a strong constitutive promoter (GPD*)* to drive expression of *SSA4*, we
109 increased the already elevated Ssa4 protein levels in an *ssa1*Δ *ssa2*Δ mutant (16) (fig. S1A)
110 and found that such overproduction of Ssa4 partially suppressed heat sensitivity (fig. 1A). Cells
111 lacking both Ssa1 and Ssa2 accumulate misfolded proteins and protein aggregates already
112 during exponential growth at 30°C, without any applied stress or increased age (16). Using the
113 misfolding proteins guk1-7-GFP and gus1-3-GFP (17), as well as the metacaspase Mca1-
114 GFP, shown to bind and manage protein aggregates (18), as reporters for protein aggregate
115 formation, we could confirm that the *ssa1*Δ *ssa2*Δ mutant accumulated protein aggregates at
116 exponential growth at 30°C to a higher degree than WT cells (fig. 1B, C). Intriguingly,
117 overproduction of Ssa4 suppressed the accumulation of protein aggregates as seen by these
118 three read-outs (fig. 1B, C) and were supported biochemically as Ssa4 overproduction reduced
119 the amounts of insoluble proteins in cells lacking Ssa1/2 (fig. 1D). The suppression of
120 aggregate formation at 30°C was not dependent on the disaggregase Hsp104, as
121 demonstrated with guk1-7-GFP (fig. S1B).

122 Another marker of protein aggregates is the small heat shock protein Hsp42, which itself is
123 required for sorting proteins into peripheral aggregates (19). Like for guk1-7, gus1-3 and Mca1,
124 we found that Hsp42 resided in aggregates already during exponential growth at 30°C in the
125 *ssa1*Δ *ssa2*Δ mutant, which could be detected through immunofluorescence using antibodies
126 against wild type Hsp42. (fig. 1E, S1C). Overproduction of Ssa4 efficiently reduced Hsp42 foci
127 formation in *ssa1*Δ *ssa2*Δ cells (fig. 1E, S1C). Thus, the data support the notion that aggregate
128 formation, including deposition of Hsp42 into peripheral aggregates, in cells lacking Ssa1/2
129 can be suppressed by overproducing Ssa4.

130 Apart from being required for mitigating protein aggregation, Ssa1/2 are also essential for the
131 coalescence of many (3 or more) small aggregates into fewer, larger inclusions upon heat
132 stress (16, 20, 21). We found that Ssa4 overproduction restored the ability of *ssa1*Δ *ssa2*Δ
133 cells to form fewer (1 to 2 foci per cell) inclusions of guk1-7-GFP after heat shock treatment
134 (fig. 1F, S1D, movies S1-3), suggesting that Ssa4 has a role also in the spatial quality control
135 of misfolded proteins in the absence of Ssa1/2.

136 **Ssa4 overproduction facilitates protein degradation in the absence of Ssa1 and Ssa2**.
137 The ability of Ssa4 to mitigate the accumulation of protein aggregates suggest that Ssa4 has
138 a role in the protection against protein aggregate formation and/or the resolution of such
139 aggregates. One strategy for reducing the amount of misfolded proteins in the cytosol is protein
140 degradation by the ubiquitin-proteasome system (UPS) (22). The ΔssCPY*-Leu2-myc
141 (ΔssCL*) construct, which is stabilized in cells with impaired proteasomal degradation and thus
142 confers increased growth on medium lacking leucine, has been used as a read-out for protein
143 degradation by the UPS (16, 23). As previously reported, cells containing the ΔssCL* construct
144 and lacking either Ssa1/2 or the E3 ubiquitin ligase Ubr1 grow better on plates without leucine
145 than wild type cells harboring ΔssCL*. Here, we found that overproduction of Ssa4 restored
146 ΔssCL* degradation in *ssa1*Δ *ssa2*Δ mutant cells, as judged by their poor growth on LEU-
147 plates (fig. 2A). We further confirmed that Ssa4 promotes degradation of misfolded proteins
148 by monitoring the degradation of ΔssCPY*-GFP (ΔssCG*) (24-27) after inhibition of translation
149 by cycloheximide. ΔssCG was stabilized in the *ssa1*Δ *ssa2*Δ mutant and overproduction of
150 Ssa4 destabilized ΔssCG* in the strain lacking Ssa1/2 (fig 2B, C). However, it is unclear if the
151 effect of Ssa4 on protein degradation alone can fully explain the pronounced effect of this
152 chaperone on mitigating aggregate formation (fig. 1B-E).

153 **Ssa4 overproduction does not efficiently promote resolution of heat induced protein**
154 **aggregates in the absence of Ssa1/2.** Resolution of protein aggregates involves the
155 disaggregase Hsp104, which is recruited to protein aggregates in an Ssa1/2-dependent
156 manner (9, 10). Ssa4-GFP localizes to sites of protein aggregation also in the absence of

157 Ssa1/2, and co-localizes with Mca1-RFP, a factor known to localize to proteins aggregates
158 (18), at those sites of aggregation (fig. 3A). Tagging Ssa4 with GFP did not inhibit growth of
159 *ssa1*Δ *ssa2*Δ cells (fig. S1F) demonstrating that the GFP-tag did not disrupt the function of
160 Ssa4 since the loss of *SSA4* in an *ssa1*Δ *ssa2*Δ background is lethal (1). Even though Ssa4
161 localized to protein aggregates, Ssa4 overproduction did not restore the recruitment of GFP-
162 Hsp104 to protein aggregates in cells lacking Ssa1/2 (fig. 3B, C). Consistently, increased levels
163 of Ssa4 did not fully restore protein aggregate clearance, measured as per cent of Ssa1/2-
164 deficicent cells displaying protein foci of the misfolded guk1-7-GFP after a heat shock (fig. 3D,
165 S1D). This was further confirmed by measuring the GFP intensity ratio between individual foci
166 and the cytosol during recovery (fig. 4A, mov. S1-3) by time-lapse microscopy. This analysis
167 captures the processes in which misfolded proteins are removed from foci, either through
168 disaggregation and refolding and/or degradation. We found that the intensity of guk1-7-GFP
169 foci in the wild type cells was steadily decreasing during recovery in a linear fashion (fig. 3E,
170 left panel, mov. S1). In contrast, there was no such decline in foci intensity in the Ssa1/2 double
171 mutant (fig. 3E, middle panel, mov. S2). Overproducing Ssa4 in the double mutant only partially
172 restored loss of foci intensity in the Ssa1/2 double mutant and the kinetics of the intensity loss
173 was not linear as in wild type cells (fig. 3E, right panel, mov. S3), which hints at a potentially
174 different mechanism underlying the resolution of the foci in these cells (fig 3E, mov. S1-3).
175 Also, as shown in figure S1B, the reduction in aggregate levels achieved by Ssa4
176 overproduction was not dependent on Hsp104.

177 **Exchanging the nucleotide binding domain (NBD) of Ssa4 allows recruitment of GFP-**
178 **Hsp104 to protein aggregates.** The NBD domain of the *E. coli* Hsp70, DnaK, has been shown
179 to interact with ClpB, a protein of the Hsp100 subfamily and this interaction is important for
180 proper clearance of protein aggregates (28). Similar findings of Hsp70-Hsp100 interactions
181 have been found in *in vitro* studies of yeast-derived Hsp70 and Hsp100 (29, 30), and the IB
182 and IIB ATPase subdomains of the Hsp70 NBD have been pinpointed as the key elements for
183 such interaction between Hsp70 and Hsp104 (30). In order to further elucidate the structure-

184 function relationship between Hsp70 and Hsp104 in aggregate recruitment, we generated
185 chimeric proteins in which each of the three domains (NBD, SBD, or CTD) of Ssa4 was
186 replaced by the Ssa1 counterpart (fig. 4A). This resulted in three different versions of Ssa4,
187 each with one Ssa1-originating domain (NBDsw = NBD swapped Ssa4, SBDsw = SBD
188 swapped Ssa4, CTDsw = CTD swapped Ssa4), that were cloned into centromeric plasmids
189 under the control of the GPD promoter. Introducing either of the three chimeric proteins
190 conferred a robust increase in total Hsp70 protein levels in the *ssa1*Δ *ssa2*Δ background (fig.
191 S2A) and all suppressed the heat sensitivity of the *ssa1*Δ *ssa2*Δ mutant to the same extent as
192 introducing either the wild type *SSA1* or *SSA4* alleles (fig. S2B). We were able to confirm that
193 GFP-Hsp104 recruitment to aggregates was rescued in the *ssa1*Δ *ssa2*Δ background with the
194 plasmid carrying the wild type *SSA1* allele, while the plasmid with *SSA4,* as expected*,* failed
195 to do so (fig. 4B, C). Interestingly, in cells lacking Ssa1/2, the chimeric version of Ssa4 with
196 the nucleotide binding domain from Ssa1 (pNBDsw) was as effective as Ssa1 in the
197 recruitment of GFP-Hsp104 to protein aggregates (fig. 4B, C). No differential effect on the
198 recruitment of GFP-Hsp104 to aggregates was observed when the different alleles were
199 introduced in the WT background (fig. S2C, D). From this data, we conclude that the nucleotide
200 binding domain of Ssa1 is involved in the recruitment of Hsp104 to protein aggregates and that
201 there is a functional difference between the NBDs of Ssa1 and Ssa4. This is in line with *in vitro*
202 data that pinpoint the NBD domain of DnaK as the site of interaction with ClpB in *E. coli* (28).

203 **Formation of ring-like aggregates around the nucleolus is Ssa1/2-dependent and cannot**
204 **be restored by Ssa4 overproduction.** It has been shown previously that the J-protein Sis1
205 and Ssa2 accumulate in partial ring-like structures around the site of ribosomal RNA
206 transcription and ribosome biogenesis in the nucleolus during heat shock of yeast cells (16,
207 31), which may be structures akin to those formed due to phase transitions in the nucleolus of
208 mammalian cells subjected to heat stress (32). Using the protein Sik1/Nop56 as a nucleolar
209 reporter (33, 34) and guk1-7 as an aggregate reporter, we found that misfolded proteins also
210 organize into perinucleolar ring structures upon heat shock (fig. 5A, B, mov. S1). The structures

211 persisted through recovery (fig. 5A, C) and eventually reformed into foci that were the last type
212 of guk1-7-GFP aggregates to be resolved after heat shock (mov. S1). Loss of Ssa1/2 inhibited
213 the formation of such structures (fig. 5, mov. S2), while other types of nuclear aggregates were
214 still formed (fig. 5A). The formation of such guk1-7-GFP rings could not be restored by
215 overproducing Ssa4 (fig. 5, mov. S3), and Ssa4-GFP does not organize into such structures
216 upon heat shock (fig. 3A), in contrast to what has been shown previously with Ssa2-GFP (16).
217 Deleting *HSP104* did not abolish the formation of the nucleolar ring-like aggregates, but
218 instead made them more stable during recovery (mov. S4). However, Hsp104 itself does not
219 associate with these structures in the nucleolus (fig. 3B, (31)). Thus, the nucleolar ring-like
220 protein aggregates formed during heat shock are dependent upon Ssa1 and/or Ssa2 to form
221 and Ssa4 cannot compensate for the lack of these chaperones in such aggregate formation.

222 **Ssa4 overproduction fully restores lifespan of short-lived *ssa1*Δ *ssa2*Δ mutant cells.**

223 A key question related to PQC and aging is whether it is more important to prevent the
224 formation of aberrant protein conformers, such as aggregates, or to maintain the ability to clear
225 the cells from such aggregates as they form. The differential effects of Ssa4 on aggregate
226 formation and clearance allowed us to approach this question. Specifically, we tested the effect
227 of Ssa4 overproduction on replicative lifespan in cells lacking Ssa1/2 as such overproduction
228 restores folding and degradation of misfolded proteins, mitigates the formation of aggregates,
229 and reinstates inclusion formation, while leaving the cells deficient in the clearance of stress-
230 induced aggregates. Intriguingly, the short lifespan of the *ssa1*Δ *ssa2*Δ mutant was completely
231 restored by Ssa4 overproduction (fig. 6A), suggesting that Hsp104-dependent protein
232 disaggregation is not required to ensure longevity if the degradation and cytosolic spatial
233 quality control mechanisms of the cell are functional.
234

235 **DISCUSSION**

236 In this paper we have established that ectopically elevating Ssa4 levels in cells lacking the
237 major cytosolic Hsp70 chaperones Ssa1 and Ssa2 can (i) suppress the heat sensitivity (fig.
238 1A), (ii) counteract protein aggregate accumulation (fig. 1B-E, 6B, S1B), (iii) improve the
239 coalescence of aggregates (fig. 1F, 6B, S1D), (iv) boost degradation of misfolded proteins (fig.
240 2A-C, 6B) and (v) restore lifespan (fig. 6A). In contrast, Ssa4 overproduction could not
241 efficiently restore Hsp104 recruitment to aggregates and therefore, aggregate clearance
242 remained slow in cells lacking Ssa1/2 (fig. 3B-E, S1E, 6B). This specific inability of Ssa4 to
243 recruit Hsp104 to aggregates appears linked to its nucleotide binding domain, as exchanging
244 this domain to that of Ssa1 fully bestowed Ssa4 with the ability to recruit Hsp104 to misfolded
245 and aggregated proteins (fig. 4B, C). Notably, the previously identified residues in the NBD
246 domain of Ssa1 that have been shown to be important in Ssa1-Hsp104 interactions (L48, Q56,
247 R255, R259, D282, G287 and D289 (30)) are all present in Ssa4 (fig. S2E). If the functional
248 difference between the NBDs of Ssa1 and Ssa4 demonstrated here is due to a difference in
249 the direct interaction between the Ssa in question and Hsp104, or a secondary effect of
250 differential interactions between the NEF partners that compete for the same binding sites (28,
251 30) remain to be elucidated.

252 We found also that a nucleolus-associated ring-like structure of the misfolding protein guk1-7-
253 GFP forms upon heat shock and requires Ssa1 and 2 for its formation. Like for aggregate
254 clearance, the formation of this structure cannot be restored by overproduction of Ssa4 in the
255 Ssa1/2 double mutant and the lack of Hsp104 stabilizes the structure after it has formed (mov.
256 S1). A similar structure has been shown before by Öling *et al.* with the use of GFP-tagged
257 Ssa2 in heat shocked cells (16) but, interestingly, we did not see a similar accumulation pattern
258 using Ssa4-GFP in the same conditions (fig 3A). This strengthens the observation that there
259 are functions of Ssa1 or 2 that Ssa4 simply fails to perform. These ring-like structures in the
260 nucleolus of yeast could be a counterpart or analogue to the phase-separated nucleolar

261 compartment for misfolded nuclear proteins described in human embryonic kidney (HEK) 293T
262 cells (32).

263 A somewhat surprising finding of this work is that Ssa4 overproduction restored inclusion
264 formation in cells lacking Ssa1/2 as Hsp104 is not recruited to aggregates in these cells.
265 Hsp104 has been shown previously to be required for formation of inclusions (20, 35-38) but
266 the data herein indicates that the recruitment of Hsp104 to aggregates may not be a
267 prerequisite for such inclusion formation. Alternatively, inclusion formation in cells lacking
268 Ssa1/2 and overproducing Ssa4 might follow a different route than the one requiring Hsp104
269 in wild type cells and could possibly lead to differences in spatial locations of inclusions. It
270 should be noted that the role of Hsp104 in longevity assurance is somewhat ambiguous; on
271 the one hand cells lacking Hsp104 age prematurely (39) and lifespan extension by
272 overproducing the metacaspase Mca1 requires Hsp104 (18). On the other hand Hsp104
273 overproduction on its own does not affect lifespan (40) and lifespan extension by duplicating
274 the gene, *TSA1,* encoding a peroxiredoxin important for Hs70 recruitment to oxidatively
275 damaged proteins, is only marginally affected by deleting *HSP104* (41). In the same vein, there
276 is evidence that aggregation management and protein quality control activities are different
277 during heat shock and ageing (41), and our results here strengthen that idea, since we have
278 shown that not all mechanisms in play during and after heat shock recovery (fig. 3D, 5, S1E)
279 need to be restored in order to maintain a normal life span (fig. 6A), even though they might
280 be necessary for survival at high temperatures (fig. 1A).

281 While it is clear that Ssa4 is able to compensate for Ssa1/2 in several aspects of PQC and
282 aging, it is also evident that mechanistic differences have evolved within this group of proteins
283 (fig. 6B). Elucidating the individual characteristics of proteins within the same chaperone family
284 may shed light on alternative pathways, such as Hsp104-independent protein inclusion
285 formation and/or protein disaggregation, which will broaden our overall view of different cellular
286 processes related to longevity and proteostasis.

287 **EXPERIMENTAL PROCEDURES**

288 **Strains and growth conditions.** Strains, plasmids, and primers used in this study are listed
289 in Supplementary Tables S1. Strains used in this study are derived from S288C genetic
290 backgrounds. Strains were grown and manipulated by using standard techniques (42). For
291 growth in rich media, strains were grown in yeast extract/peptone/dextrose (YPD) with 2 %
292 glucose. Cells grown in synthetic defined medium were typically grown with yeast nitrogen
293 base plus ammonium sulfate, synthetic complete drop-out mixture and 2% glucose.

294 **Strain construction.** The GPD promoter was amplified from the pYM-N15 plasmid and
295 incorporated upstream of the *SSA4* ORF via homologous recombination in the WT and *ssa1*Δ
296 *ssa2*Δ backgrounds. Deletion mutants were constructed either by PCR-mediated knockout or
297 sporulation. Transformants and dissected spores were verified by PCR. Plasmids with
298 misfolding GPD-tagged proteins (pguk1-7GFP and pgus1-3GFP*)* were linearized with
299 restriction enzymes (NsiI) and integrated at the *HIS* locus via homologous recombination. The
300 three chimeric *SSA4-SSA1* alleles were constructed (GenScript Biotech Corporation, Nanjing,
301 China) and cloned into carrier vectors. The constructs were then amplified with homologous
302 sequences at the 5' and 3'-ends to allow for homologous recombination into the pRS415
303 vector. The *SSA1* and *SSA4* alleles were amplified from the BY4741 strain with the same
304 homologous sequences. The pRS415 vector was digested with XbaI and HindIII (Thermo
305 Fisher Scientific) and the plasmids were recombined with the constructs in wild type yeast and
306 then extracted and transformed into *E. coli* to allow for plasmid production. The final vectors
307 were digested with HindIII and SacI (Thermo Fisher Scientific) for insert size control and then
308 sequenced for verification prior to transformation into the intended host strains.

309 **Heat-sensitivity assay**. Cultures were grown to mid-exponential phase at 30°C, and serially
310 diluted (tenfold) to an optical density (38) of A_{600} = 10^{-1}–10^{-5}. Dilutions were spotted onto YPD
311 or synthetic defined medium plates and incubated at the indicated temperatures for 2-3 days
312 prior to imaging.

313 **Replicative lifespan analysis.** Lifespan analyses were performed as previously described
314 (Kaeberlein et al, 1999, Erjavec et al, 2007). Briefly, cells were grown overnight in YPD, diluted,
315 plated, and allowed to recover on YPD plates before being assayed for RLS which was
316 performed using a micromanipulator (Singer instruments) to remove daughters from mother
317 cells. Replicative lifespan analysis was performed independently at least three times for each
318 strain. Statistical analysis was performed using unpaired Mann-Whitney U-test in GraphPad
319 Prism® 7.01.

320 **Stress-treatments used to induce protein aggregation.** Cells were grown to mid-
321 exponential phase at 30°C and then shifted to the indicated temperatures. For visualization of
322 protein aggregate formation, cells were kept at indicated temperatures and samples were
323 taken over time, and cells were scored as either having no or one or more protein aggregate
324 foci. For resolution of protein aggregates and aggregate coalescence after heat shock, cells
325 were shifted back to 30°C after heat shock and samples were taken over time. For the
326 resolution of protein aggregate foci cells were scored as either having none or one or more
327 protein aggregate foci. The OD of each culture was measured at each sampling time point for
328 normalization. Protein aggregate coalescence/inclusion formation during recovery was scored
329 in three categories: foci-free (0 foci), class I/II (1-2 foci) and class III (3 or more foci). All cells
330 in the foci-free category was omitted and the remaining cells with at least one foci were used
331 in the analysis. Images were analyzed with ImageJ (Fiji package) (43). Statistical analyses
332 were performed in GraphPad Prism® 7.01 (GraphPad Software LLC) and Microsoft® Excel®
333 2016 (Microsoft Corporation).

334 **GFP-Hsp104 expression from *GAL1*-promoter.** Cultures were grown over the day in
335 synthetic defined medium lacking histidine (CSM-HIS) or leucine and histidine (CSM-LEU-HIS)
336 with 2% galactose. Cultures were resuspended in fresh medium with 2% galactose and grown
337 to mid-exponential phase over the night. Sample of mid-exponential phase cells were taken
338 before and after heat shock (42 °C, 30 minutes).

339 **DAPI-stain of live cells.** Cells were cultured, treated and sampled as described above. Prior
340 to imaging, 10 µg/ml of 4′,6-diamidino-2-phenylindole (DAPI) in MilliQ H_2O was added to each
341 cell sample and incubated in darkness for 5 minutes before pelleting by centrifugation and
342 subsequent imaging.

343 **Fluorescence microscopy.** Images were obtained using a conventional fluorescence
344 microscope, a Zeiss Axio Observer.Z1 inverted microscope with Apotome and Axiocam 506
345 camera, and a Plan-Apochromat 100x/1.40 Oil DIC M27 objective.

346 **Isolation of insoluble protein.** Insoluble protein aggregates were isolated as described (Rand
347 and Grant, 2006), with minor adjustments. The protocol was scaled up to suit the harvesting
348 of 35 A_{600} units of cells. Pefabloc SC (Roche) was used instead of phenylmethylsulfonyl
349 fluoride in the lysis buffer. After freezing and thawing the cells they were immediately disrupted
350 by a minibead beater (Fastprep) at 5.5 m/s for 4x30 sec at 4°C. Cells were kept on ice for 5
351 min between each beating. Removal of intact cells was accomplished by centrifugation at 1180
352 x g for 15 min. Protein concentration was determined using Pierce 660 nm Assay Reagent
353 (Thermo Scientific) and adjusted before isolation of protein aggregates as well as verified by
354 running reduced samples on Criterion XT Precast Gel 4-12% Bis-Tris (BioRad) and staining
355 with Coomassie Brilliant Blue R-250 staining solution (BioRad). The subsequent
356 centrifugations were all done at 21130 x g for 20 min. Insoluble fractions were resuspended in
357 detergent washes by 5 x 5 sec sonication at amp 40 with 15 sec rest between intervals using
358 Q700 Sonicator (QSonica, LLC. Newtown, USA). The insoluble fractions were added to
359 reduced protein loading buffer, loaded on Criterion XT Precast Gel 4-12% Bis-Tris (BioRad)
360 and visualized by silver staining with Pierce® Silver Stain Kit (Thermo Scientific).

361 **Growth test for cells expressing ΔssCL*.** Overnight pre-cultured cells were diluted to an
362 O.D. of A_{600}=0.5, spotted in a fivefold dilution series on CSM-URA or CSM -URA -LEU plates
363 and incubated at 30°C for 3–4 days.

364 **Protein extraction, gel electrophoresis and western blot.** Cells were cultured overnight and
365 then diluted down to an O.D. of A_{600}=0.1 and allowed to grown to an O.D. of A_{600}=0.5 before
366 harvest. For denaturing gel electrophoresis, proteins were extracted as described by (44) with
367 a few modifications. Briefly, 1 O.D. unit of cells were lysed in 200 µl of 0.2 M NaOH for 20
368 minutes on ice followed by centrifugation for 1 minute at 13000 rpm, 4 °C. The protein pellet
369 was resuspended in 50 µl per O.D. unit of cells in a 1X Laemmli/8 M Urea/ 2.5 % β-
370 mercaptoethanol sample buffer and incubated for 10 minutes at 70 °C prior to SDS-PAGE
371 using 4-12 % Bis-Tris gels (Invitrogen NuPAGE®, Thermo Scientific) in a MOPS buffer
372 (Invitrogen NuPAGE®, Thermo Scientific) according to the manufacturers instruction. The gels
373 were blotted onto an Immobilion-P PVDF membrane, 0.45 µm pore size, (MERCK Millipore)
374 in a Tris-glycine-methanol transfer buffer overnight and detected with the following antibodies:
375 1:5000 monoclonal mouse anti-Hsp70 [C92F3A-5] (Abcam Cat# ab47455, RRID:AB_881520)
376 (abcam), 1:15000 monoclonal mouse anti-Pgk1 (Thermo Fisher Scientific Cat# 459250,
377 RRID:AB_2532235). The primary antibodies were detected using 1:20000 goat anti-mouse or
378 rat IgG (H+L) IRDye® 680LT or 800CW (mouse 680LT: LI-COR Biosciences Cat# 926-68020,
379 RRID:AB_10706161, mouse 800CW: LI-COR Biosciences Cat# 926-32210,
380 RRID:AB_621842, rat 680LT: LI-COR Biosciences Cat# 926-68029, RRID:AB_10715073, rat
381 800CW: LI-COR Biosciences Cat# 926-32219, RRID:AB_1850025), the blots were scanned
382 using the Odyssey® Near Infra-red imaging system (LI-COR) and the images were analyzed
383 using ImageJ.

384 **Cycloheximide chase.** Logarithmically growing cells expressing ΔssCG* were harvested and
385 resuspended in complex media. Protein translation was shut off by addition of cycloheximide
386 (PubChem CID: 6197) (0.5 mg/ml final concentration). 2 O.D. units of cells were taken at
387 indicated time-points, protein samples were prepared with minor changes as described above.
388 8 M Urea loading dye was supplemented with complete protease inhibitor (Roche). 100 µl Urea
389 loading dye were used to resuspend cell pellet after NaOH treatment. 15 µl of the protein
390 extracts were loaded on a 4-12% gradient 26 well Criterion XT Bis-Tris Protein gel (Bio-Rad).

391 Gels were transferred on PVDF membrane. Membranes were blocked with Odyssey blocking
392 buffer (Li-COR) followed by incubation with antibodies specific for GFP (mouse monoclonal
393 anti-GFP [7.1 and 13.1] (Sigma-Aldrich Cat# 11814460001, RRID:AB_390913)) and Tub1 (rat
394 monoclonal anti-tubulin alpha, (Bio-Rad Cat# MCA77G, RRID:AB_325003)) (1:10000 dilution
395 each in PBS-T). The primary antibodies were detected and the membranes scanned as
396 described above.

397 **Immunofluorescence.** Cells were fixed in 9 parts 0.1 mM KPO_4, 500 mM $MgCl_2$ and 1 part 37
398 % formaldehyde for 1h at 30 °C, washed once in 0.1 M KPO_4, 500 µM $MgCl_2$ and once in 0.1
399 M KPO_4, 500 µM $MgCl_2$, 0.1 M Sorbitol (sorbitol solution). Spheroplasts were prepared by
400 incubating approximate 3 O.D. units of fixed cells at 35 °C with 0.6 mg/ml Zymolase in sorbitol
401 solution. Spheroplasts were gently washed in sorbitol solution before being spotted on
402 polylysin-coated slides and permeabilized swiftly with 1 % Triton X-100 in BSA-PBS (1 %
403 BSA). Blocking was done in BSA-PBS. To avoid unspecific binding of primary antibody,
404 polyclonal rabbit anti-Hsp42, 1:2000 (gift from Prof. Johannes Buchner, Germany) in PBS-
405 BSA, was pre-incubated on a western blot membrane with transferred BY4741 *hsp42Δ::kanMx*
406 lysate for 1.5 h at room temperature (RT) before antibody solution was added to slides. Slides
407 were incubated with 1:500 goat anti-Rabbit Alexa488 (Thermo Fisher Scientific Cat# A-11034,
408 RRID:AB_2576217), washed, incubated with 1 µg/ml DAPI for 10 min at RT and washed
409 before mounting media was added and slides were sealed with nail polish. Mounting media
410 was prepared by adding 100 mg p-phehylenediamine in 10 ml PBS, pH was adjusted to 8.0
411 with 0.5M Sodium carbonate buffer (pH 9.0) and volume was brought to 100 ml by addition of
412 glycerol.

413 **Time lapse microscopy.** Cells were grown in YPD medium to an $O.D._{600}$ between 0.3 and
414 0.5 at 30 °C after which they were heat shocked at 42 °C for 30 minutes. The heat shocked
415 samples were washed with PBS and then placed onto agar pads with complete synthetic
416 media supplemented with YNB and 2 % glucose mounted on microscope slides. The
417 samples were imaged at 30 °C on a Zeiss Axio Observer.Z1 inverted microscope with

418 Apotome and Axiocam 506 camera, and a Plan-Apochromat 100x/1.40 Oil DIC M27
419 objective, with the following incubation equipment to maintain temperature: TempModule S1
420 (Zeiss), Y module S1 (Zeiss), Temperable insert S1 (Zeiss), Temperable objective ring S1
421 (Zeiss), and Incubator S1 230 V (Zeiss). 10 *Z*-stack images were captured at four distinct
422 coordinates every 10 minutes for 120 minutes. The time lapse captures were processed in
423 ImageJ (Fiji package) (43) using the Bleach Correction with Simple Ratio (45) and the Linear
424 Stack Alignment with SIFT (46) plugins. The analysis was performed in ImageJ by measuring
425 the Integrated Density ($IntDen_{ROI}$) and Area (A_{ROI}) of a focus and a same-sized spot of the
426 cytoplasm for each focus and time point. Mean fluorescence measurements (M_B) were also
427 taken of the cell-free background. The corrected cellular compartment fluorescence for each
428 focus and associated foci-free cytosol was then calculated for each focus and time point with
429 the following equation: $IntDen_{ROI} – (A_{ROI} * M_B)$. After that, the ratio between the individual
430 focus and corresponding cytosol was calculated for each time point. The linear regression
431 and statistical analysis were carried out using GraphPad Prism® 7.01 (GraphPad Software
432 LLC).

433 **ACKNOWLEDGEMENTS**

434 The authors would like to thank Johannes Buchner for the generous gift of the rabbit anti-
435 Hsp42 antibody, Charles Boone for strains and Per Widlund for the gus1-3-GFP and guk1-7-
436 GFP plasmids used in this study.

437 **REFERENCES**

438 1. Werner-Washburne M, Stone DE, Craig EA. Complex interactions among members
439 of an essential subfamily of hsp70 genes in Saccharomyces cerevisiae. Mol Cell Biol.
440 1987;7(7):2568-77.
441 2. Mayer MP, Bukau B. Hsp70 chaperones: cellular functions and molecular
442 mechanism. Cell Mol Life Sci. 2005;62(6):670-84.

443 3. Schmid D, Baici A, Gehring H, Christen P. Kinetics of molecular chaperone action.
444 Science. 1994;263(5149):971-3.
445 4. McCarty JS, Buchberger A, Reinstein J, Bukau B. The role of ATP in the functional
446 cycle of the DnaK chaperone system. J Mol Biol. 1995;249(1):126-37.
447 5. Zhu X, Zhao X, Burkholder WF, Gragerov A, Ogata CM, Gottesman ME, et al.
448 Structural analysis of substrate binding by the molecular chaperone DnaK. Science.
449 1996;272(5268):1606-14.
450 6. Sharma D, Masison DC. Hsp70 structure, function, regulation and influence on yeast
451 prions. Protein Pept Lett. 2009;16(6):571-81.
452 7. Kampinga HH, Craig EA. The HSP70 chaperone machinery: J proteins as drivers of
453 functional specificity. Nat Rev Mol Cell Biol. 2010;11(8):579-92.
454 8. Rampelt H, Mayer MP, Bukau B. Nucleotide exchange factors for Hsp70 chaperones.
455 Methods Mol Biol. 2011;787:83-91.
456 9. Glover JR, Lindquist S. Hsp104, Hsp70, and Hsp40: a novel chaperone system that
457 rescues previously aggregated proteins. Cell. 1998;94(1):73-82.
458 10. Winkler J, Tyedmers J, Bukau B, Mogk A. Hsp70 targets Hsp100 chaperones to
459 substrates for protein disaggregation and prion fragmentation. J Cell Biol. 2012;198(3):387-
460 404.
461 11. Hasin N, Cusack SA, Ali SS, Fitzpatrick DA, Jones GW. Global transcript and
462 phenotypic analysis of yeast cells expressing Ssa1, Ssa2, Ssa3 or Ssa4 as sole source of
463 cytosolic Hsp70-Ssa chaperone activity. BMC Genomics. 2014;15:194.
464 12. Sharma D, Martineau CN, Le Dall MT, Reidy M, Masison DC, Kabani M. Function of
465 SSA subfamily of Hsp70 within and across species varies widely in complementing
466 Saccharomyces cerevisiae cell growth and prion propagation. PLoS One. 2009;4(8):e6644.
467 13. Schwimmer C, Masison DC. Antagonistic interactions between yeast [PSI(+)] and
468 [URE3] prions and curing of [URE3] by Hsp70 protein chaperone Ssa1p but not by Ssa2p.
469 Mol Cell Biol. 2002;22(11):3590-8.

470 14. Boorstein WR, Craig EA. Structure and regulation of the SSA4 HSP70 gene of
471 Saccharomyces cerevisiae. J Biol Chem. 1990;265(31):18912-21.
472 15. Craig EA, Jacobsen K. Mutations of the heat inducible 70 kilodalton genes of yeast
473 confer temperature sensitive growth. Cell. 1984;38(3):841-9.
474 16. Oling D, Eisele F, Kvint K, Nystrom T. Opposing roles of Ubp3-dependent
475 deubiquitination regulate replicative life span and heat resistance. EMBO J. 2014;33(7):747-
476 61.
477 17. Comyn SA, Young BP, Loewen CJ, Mayor T. Prefoldin Promotes Proteasomal
478 Degradation of Cytosolic Proteins with Missense Mutations by Maintaining Substrate
479 Solubility. PLoS Genet. 2016;12(7):e1006184.
480 18. Hill SM, Hao X, Liu B, Nystrom T. Life-span extension by a metacaspase in the yeast
481 Saccharomyces cerevisiae. Science. 2014;344(6190):1389-92.
482 19. Specht S, Miller SB, Mogk A, Bukau B. Hsp42 is required for sequestration of protein
483 aggregates into deposition sites in Saccharomyces cerevisiae. J Cell Biol. 2011;195(4):617-
484 29.
485 20. Escusa-Toret S, Vonk WI, Frydman J. Spatial sequestration of misfolded proteins by
486 a dynamic chaperone pathway enhances cellular fitness during stress. Nat Cell Biol.
487 2013;15(10):1231-43.
488 21. Malinovska L, Kroschwald S, Munder MC, Richter D, Alberti S. Molecular chaperones
489 and stress-inducible protein-sorting factors coordinate the spatiotemporal distribution of
490 protein aggregates. Mol Biol Cell. 2012;23(16):3041-56.
491 22. Tanaka K. The proteasome: overview of structure and functions. Proc Jpn Acad Ser
492 B Phys Biol Sci. 2009;85(1):12-36.
493 23. Eisele F, Wolf DH. Degradation of misfolded protein in the cytoplasm is mediated by
494 the ubiquitin ligase Ubr1. FEBS Lett. 2008;582(30):4143-6.
495 24. Medicherla B, Kostova Z, Schaefer A, Wolf DH. A genomic screen identifies Dsk2p
496 and Rad23p as essential components of ER-associated degradation. EMBO Rep.
497 2004;5(7):692-7.

498 25. Park SH, Bolender N, Eisele F, Kostova Z, Takeuchi J, Coffino P, et al. The
499 cytoplasmic Hsp70 chaperone machinery subjects misfolded and endoplasmic reticulum
500 import-incompetent proteins to degradation via the ubiquitin-proteasome system. Mol Biol
501 Cell. 2007;18(1):153-65.
502 26. Prasad R, Kawaguchi S, Ng DT. A nucleus-based quality control mechanism for
503 cytosolic proteins. Mol Biol Cell. 2010;21(13):2117-27.
504 27. Park SH, Kukushkin Y, Gupta R, Chen T, Konagai A, Hipp MS, et al. PolyQ proteins
505 interfere with nuclear degradation of cytosolic proteins by sequestering the Sis1p chaperone.
506 Cell. 2013;154(1):134-45.
507 28. Rosenzweig R, Moradi S, Zarrine-Afsar A, Glover JR, Kay LE. Unraveling the
508 mechanism of protein disaggregation through a ClpB-DnaK interaction. Science.
509 2013;339(6123):1080-3.
510 29. Lee J, Kim JH, Biter AB, Sielaff B, Lee S, Tsai FTF. Heat shock protein (Hsp) 70 is an
511 activator of the Hsp104 motor. Proceedings of the National Academy of Sciences of the
512 United States of America. 2013;110(21):8513-8.
513 30. Doyle SM, Shastry S, Kravats AN, Shih YH, Miot M, Hoskins JR, et al. Interplay
514 between E. coli DnaK, ClpB and GrpE during protein disaggregation. J Mol Biol.
515 2015;427(2):312-27.
516 31. Feder ZA, Ali A, Singh A, Krakowiak J, Zheng X, Bindokas VP, et al. Subcellular
517 localization of the J-protein Sis1 regulates the heat shock response. biorXiv.
518 2020;2020.04.02.022491 [Preprint] (cited 2020 Apr 27):Availiable at:
519 https://www.biorxiv.org/content/10.1101/2020.04.02.022491v1.
520 32. Frottin F, Schueder F, Tiwary S, Gupta R, Korner R, Schlichthaerle T, et al. The
521 nucleolus functions as a phase-separated protein quality control compartment. Science.
522 2019;365(6451):342-7.
523 33. Gautier T, Berges T, Tollervey D, Hurt E. Nucleolar KKE/D repeat proteins Nop56p
524 and Nop58p interact with Nop1p and are required for ribosome biogenesis. Mol Cell Biol.
525 1997;17(12):7088-98.

526 34. Lechertier T, Grob A, Hernandez-Verdun D, Roussel P. Fibrillarin and Nop56 interact
527 before being co-assembled in box C/D snoRNPs. Exp Cell Res. 2009;315(6):928-42.
528 35. Krobitsch S, Lindquist S. Aggregation of huntingtin in yeast varies with the length of
529 the polyglutamine expansion and the expression of chaperone proteins. Proc Natl Acad Sci
530 U S A. 2000;97(4):1589-94.
531 36. Spokoini R, Moldavski O, Nahmias Y, England JL, Schuldiner M, Kaganovich D.
532 Confinement to organelle-associated inclusion structures mediates asymmetric inheritance of
533 aggregated protein in budding yeast. Cell Rep. 2012;2(4):738-47.
534 37. Miller SB, Ho CT, Winkler J, Khokhrina M, Neuner A, Mohamed MY, et al.
535 Compartment-specific aggregases direct distinct nuclear and cytoplasmic aggregate
536 deposition. EMBO J. 2015.
537 38. Song J, Yang Q, Yang J, Larsson L, Hao X, Zhu X, et al. Essential genetic interactors
538 of SIR2 required for spatial sequestration and asymmetrical inheritance of protein
539 aggregates. PLoS Genet. 2014;10(7):e1004539.
540 39. Erjavec N, Larsson L, Grantham J, Nystrom T. Accelerated aging and failure to
541 segregate damaged proteins in Sir2 mutants can be suppressed by overproducing the
542 protein aggregation-remodeling factor Hsp104p. Genes Dev. 2007;21(19):2410-21.
543 40. Andersson V, Hanzen S, Liu B, Molin M, Nystrom T. Enhancing protein
544 disaggregation restores proteasome activity in aged cells. Aging (Albany NY).
545 2013;5(11):802-12.
546 41. Hanzen S, Vielfort K, Yang J, Roger F, Andersson V, Zamarbide-Fores S, et al.
547 Lifespan Control by Redox-Dependent Recruitment of Chaperones to Misfolded Proteins.
548 Cell. 2016;166(1):140-51.
549 42. Sherman F. Getting started with yeast. Methods Enzymol. 1991;194:3-21.
550 43. Schindelin J, Arganda-Carreras I, Frise E, Kaynig V, Longair M, Pietzsch T, et al. Fiji:
551 An Open-Source Platform for Biological-Image Analysis. Nature Methods. 2012;9(7):676-82.

552 44. Hwang CS, Shemorry A, Varshavsky A. Two proteolytic pathways regulate DNA
553 repair by cotargeting the Mgt1 alkylguanine transferase. Proc Natl Acad Sci U S A.
554 2009;106(7):2142-7.
555 45. Miura K, Rueden C, Hiner M, Schindelin J, Rietdorf J. ImageJ Plugin CorrectBleach.
556 2.0.2 ed: Zenodo; 2014.
557 46. Lowe DG. Distinctive Image Features from Scale-Invariant Keypoints. International
558 Journal of Computer Vision. 2004;60(2):91-110.

559

560

561 **FIGURE CAPTIONS**

562 **Figure 1. Ssa4 overproduction suppresses heat sensitivity and mitigates protein**
563 **aggregate accumulation in the absence of Ssa1/2.** A) Heat sensitivity test of wild type (WT),
564 and *ssa1*Δ *ssa2*Δ with or without *SSA4* under the control of the GPD-promoter (P_{GPD}*SSA4*).
565 The strains were serial diluted $1x10^{-1}$-$1x10^{-5}$ and incubated on YPD plates for 2 days at the
566 indicated temperatures. B) Fluorescent microscopy images of guk1-7-GFP, gus1-3-GFP and
567 Mca1-GFP in WT, *ssa1*Δ *ssa2*Δ, and *ssa1*Δ *ssa2*Δ P_{GPD}*SSA4* background at exponential
568 growth at 30 °C. C) Quantifications of B. Columns represents the mean of 3 biological
569 replicates, *n* = 200. Error bars: +/- S.D. D) Silver stained gel showing total protein input and
570 the insoluble protein fraction of WT, *ssa1*Δ *ssa2*Δ, and *ssa1*Δ *ssa2*Δ P_{GPD}*SSA4* during
571 exponential growth at 30 °C (lane 1-3) and heat shocked WT cells (38 °C for 60 minutes, lane
572 4). Bands below represent immunoblot detection of Tubulin (as a loading control). E)
573 Quantifications of Hsp42 foci in WT, *ssa1*Δ *ssa2*Δ, and *ssa1*Δ *ssa2*Δ P_{GPD}*SSA4* using Hsp42
574 immunofluorescence. Error bars: +/- S.D. F) Guk1-7-GFP foci phenotype of cells with one or
575 more foci after 30 minutes of heat shock at 42 °C and during recovery at 30 °C. Columns
576 represents the mean of 3 biological replicates, *n* = 200. White bars: 1-2 foci per cell with foci,
577 grey bars: 3 or more foci per cell with foci. Note that not all cells have foci in the later time
578 points (see fig. 3D, S1D). Error bars: +/- S.D. * denotes significant difference ($p<0.05$) from the
579 two other strains.

580 **Figure 2. Ssa4 improves degradation of CPY* in the absence of Ssa1/2.** A) Growth test of
581 cells expressing ΔssCL* in WT, *ssa1*Δ *ssa2*Δ, and *ssa1*Δ *ssa2*Δ P_{GPD}*SSA4* background. The
582 strains were grown on plates lacking leucine and uracil or uracil only (control) for 2-3 days at
583 30 °C. B) Western blot of Δ*ss*CG* with αGFP antibody after a cycloheximide chase in WT,
584 *ssa1*Δ *ssa2*Δ and *ssa1*Δ *ssa2*Δ P_{GPD}*SSA4*. Number panel represents time in minutes after
585 addition of 0.5 mg/ml cycloheximide. C) Quantification of B. Band intensities of the Δ*ss*CG*
586 band were normalized against the corresponding Tub1 band and levels at time point 0 were

587 set to 1 and graphed as the power of 10 logarithm. Error bars represent standard error of the
588 mean of three replicates. p.d.u. = procedure defined unit.

589 **Figure 3. Ssa4 overproduction cannot restore Hsp104 recruitment or protein aggregate**
590 **resolution in cells lacking Ssa1/Ssa2.** A) Fluorescent microscopy images of WT and *ssa1*Δ
591 *ssa2*Δ with Ssa4-GFP and Mca1-RFP under exponential growth at 30 °C and heat shock (42
592 °C, 30 min) White arrows denotes co-localizing foci. Dashed lines are cell outlines. B)
593 Fluorescent microscopy images of GFP-Hsp104 in WT, *ssa1*Δ *ssa2*Δ, and *ssa1*Δ *ssa2*Δ
594 P_{GPD}*SSA4* background under exponential growth at 30 °C and heat shock (42 °C, 30 minutes).
595 C) Quantifications of B. Columns represent the mean of 4 biological replicates, n = 200. White
596 bars: wild type (WT), dark grey bars: *ssa1*Δ *ssa2*Δ, and light grey bars: *ssa1*Δ *ssa2*Δ
597 P_{GPD}*SSA4*. Error bars: +/- S.D. D) Quantifications of fluorescent microscopy images of guk1-
598 7-GFP after 30 minutes of heat shock at 42 °C and during recovery at 30 °C. The panel shows
599 the percentage of cells with foci, with the level at time 0 being set to 100 %. Values were
600 normalized to the growth of the culture (measured by the optical density at 600 nm). Symbols
601 represent the mean of 3 biological replicates, n = 200. White circles: wild type (WT), dark grey
602 squares: *ssa1*Δ *ssa2*Δ, and light grey triangles: *ssa1*Δ *ssa2*Δ P_{GPD}*SSA4*. Error bars: +/- S.D.
603 E) Ratio between the GFP intensity of foci and cytoplasm in strains with guk1-7-GFP during
604 recovery from 10 to 120 minutes after heat shock (42 °C for 30 minutes). Circles represent the
605 mean ratio of the focus:cytosol intensity at each time point from 20 tracked foci in 20 cells per
606 strain (2 biological replicates), dashed area: +/- S.D. of the mean ratio, dashed lines represents
607 ratio 1:1 = no detectable foci, and the full line is the linear regression of the mean ratios. p. d.
608 u. = procedure defined units. Left panel: WT, Middle panel: *ssa1*Δ *ssa2*Δ, and Right panel:
609 *ssa1*Δ *ssa2*Δ P_{GPD}*SSA4*. The boxes underneath each graph contains the equation of the line
610 from the linear regression, the r^2 values, standard deviation of the residuals (Sy.x) and the *p*-
611 values of the runs tests performed after the regression.

612 **Figure 4. The nucleotide binding domain of Ssa1 but not Ssa4 mediates Hsp104**
613 **recruitment to misfolded and aggregated proteins.** A) Chimeric Ssa1/Ssa4 constructs used

614 in this study. NBDsw = Nucleotide Binding Domain swapped Ssa4, SBDsw = Substrate Binding
615 Domain swapped Ssa4, CTDsw = C-Terminal Domain swapped Ssa4. B) Fluorescent
616 microscopy images of GFP-Hsp104 in *ssa1*Δ *ssa2*Δ carrying the empty vector (pRS415), wild
617 type Ssa1 and Ssa4 (*pSSA1* and p*SSA4*), and each of the three chimeric versions of Ssa4
618 (p*NBD*sw, p*SBD*sw and p*CTD*sw) under exponential growth at 30 °C and heat shock (42 °C,
619 30 min). C) Quantification of cells with foci from B. Columns represent the mean of 6 biological
620 replicates, *n*=193-204. Dark grey: pRS415, white: *pSSA1*, light grey: p*SSA4,* light green:
621 p*NBDsw,* green*:* p*SBDsw*, and dark green: p*CTDsw*. Error bars: +/- S.D. ▼ symbols above
622 the bars indicate statistically significant difference from p*SSA1* calculated by two-way ANOVA
623 with multiple comparisons between the strains, with Tukey's post-hoc test, $p < 0.05$. D)
624 Western blot of co-immunoprecipitation with purified Hsp104 protein and cell extracts from
625 *ssa1*Δ *ssa2*Δ *hsp104*Δ cells producing FLAG-tagged versions of either Ssa1 (left), the NBDsw
626 (middle) or the SBDsw (right) chimaeras of Ssa4.

627 **Figure 5. guk1-7-GFP forms an Ssa1/2 ring-like structure around the nucleolus after heat**
628 **shock.** A) Fluorescent microscopy images of guk1-7-GFP, pSik1-RFP and DAPI stain in WT,
629 *ssa1*Δ *ssa2*Δ, and *ssa1*Δ *ssa2*Δ P_{GPD}*SSA4* background at control (exponential growth at 30
630 °C), heat shock (42 °C for 30 minutes) and 40 minutes post-heat shock recovery at 30 °C.
631 Dashed lines represents cellular outlines. White squares shows inserts displayed in B. Green:
632 guk1-7-GFP, magenta: Sik1-RFP, blue: DAPI. B) Zoom in of fluorescent microscopy images
633 of guk1-7-GFP and pSik1-RFP stain in WT, *ssa1*Δ *ssa2*Δ, and *ssa1*Δ *ssa2*Δ P_{GPD}*SSA4*
634 background after heat shock (42 °C for 30 minutes). Dashed lines represents cellular outlines.
635 White arrowheads indicates nucleolus-associated ring-like aggregate structure of guk1-7-GFP.
636 Green: guk1-7-GFP, magenta: Sik1-RFP. C) Quantification of percent of cells with guk1-7-
637 GFP ring-like aggregate structures that surrounds the Sik1-RFP signal as shown in A. Columns
638 represent the mean of 3 biological replicates, *n* = 114-201. White: WT, dark grey: *ssa1*Δ *ssa2*Δ*,*
639 light grey: *ssa1*Δ *ssa2*Δ P_{GPD}*SSA4*. Error bars: +/- S.D.

640 **Figure 6. Lifespan analysis and schematic representation of Ssa1 vs. Ssa4 function in**
641 **PQC.** A) Replicative lifespan of WT and *ssa1*Δ *ssa2*Δ strains with or without *SSA4* under the
642 control of the GPD-promoter (P_{GPD}*SSA4*). Numbers in parenthesis indicate the mean
643 replicative lifespan of each strain. White squares: WT (*n* = 150), Green squares: P_{GPD}*SSA4* (*n*
644 = 179), Black squares: *ssa1*Δ *ssa2*Δ (*n* = 174) and Grey squares: *ssa1*Δ *ssa2*Δ P_{GPD}*SSA4* (*n*
645 = 321). B) Ssa1/2 (blue) acts on misfolded proteins to promote refolding or degradation. In
646 addition, Ssa1/2 recruits Hsp104 (dark grey) to misfolded, aggregated proteins and aid in the
647 formation of inclusion bodies and nucleolus-associated ring-like aggregates and clearance of
648 protein aggregates. In contrast, Ssa4 (red) can in the absence of Ssa1 and 2 promote refolding
649 and degradation of misfolded proteins as well as aid in the formation of inclusion bodies but
650 does not support the formation of the nucleolus-associated aggregation compartment, nor
651 does it recruit Hsp104 as efficiently to protein aggregates or support efficient clearance of
652 aggregated proteins.

653 **SUPPLEMENTAL MOVIE CAPTIONS**

654 **Movie S1.** Time lapse microscopy of BY4741 guk1-7-GFP cells during recovery at 30 °C after
655 heatshock at 42 °C for 30 minutes. The movies show 12 images captured every 10 minutes
656 from 10 to 120 minutes after the heat shock was completed.
657
658 **Movie S2.** Time lapse microscopy of *ssa1*Δ *ssa2*Δ guk1-7-GFP cells during recovery at 30 °C
659 after heatshock at 42 °C for 30 minutes. The movies show 12 images captured every 10
660 minutes from 10 to 120 minutes after the heat shock was completed.
661
662 **Movie S3.** Time lapse microscopy of *ssa1*Δ *ssa2*Δ P_{GPD}*SSA4* guk1-7-GFP cells during
663 recovery at 30 °C after heatshock at 42 °C for 30 minutes. The movies show 12 images
664 captured every 10 minutes from 10 to 120 minutes after the heat shock was completed.
665

666 **Movie S4.** Time lapse microscopy of *hsp104*Δ guk1-7-GFP cells during recovery at 30 °C after
667 heatshock at 42 °C for 30 minutes. The movies show 12 images captured every 10 minutes
668 from 10 to 120 minutes after the heat shock was completed.

669 **SUPPLEMENTAL FIGURE CAPTIONS**

670 **Figure S1.** A) Left: Cut-outs of silver stained 2-dimensinal polyacrylamide gels showing Ssa1,
671 Ssa2 and Ssa4 in protein extracts from WT, P_{GPD}*SSA4, ssa1*Δ *ssa2*Δ and *ssa1*Δ *ssa2*Δ
672 P_{GPD}*SSA4* cells. Black arrows indicate the named proteins. Right: Quantification the gels
673 shown to the left with respect to Ssa4 levels relative to Act1. WT is set to 1. B) Quantification
674 of number of foci per cell of guk1-7-GFP in WT, *ssa1*Δ *ssa2*Δ and *ssa1*Δ *ssa2*Δ P_{GPD}*SSA4*
675 with (left) or without (right) *HSP104*. C) Fluorescent microscopy images of Hsp42 in WT, *ssa1*Δ
676 *ssa2*Δ, and *ssa1*Δ *ssa2*Δ P_{GPD}*SSA4* by anti-Hsp42 antibody detection D) Fluorescent
677 microscopy images of guk1-7-GFP cells after heat shock (42 °C for 30 minutes) and during
678 recovery at 30 °C. Shown are images representative of three biological replicates. Images
679 were generated as a maximum projection of one representative slice from a *Z*-stack using
680 ImageJ 1.50i (Rasband, 1997) with 64-bit Java 1.8.0_77. E) Heat sensitivity test of WT and
681 *ssa1*Δ *ssa2*Δ with or without GFP-tagged Ssa4.
682

683 **Figure S2.** A) Representative western blot of SDS-PAGE gel with anti-Hsp70 antibody and
684 anti-Pgk1 antibody as loading control (left). Quantification of immunoblotted SDS-PAGE gel
685 with respect to total Hsp70 (right). Values have been normalized to Pgk1 as loading control
686 and the level in WT at steady state set to 1. Bars represent one representative replicate out of
687 two. White with black dots: WT pRS415, dark grey: *ssa1*Δ *ssa2*Δ pRS415, white: *ssa1*Δ *ssa2*Δ
688 pSSA1, light grey: *ssa1*Δ *ssa2*Δ pSSA4, light green: *ssa1*Δ *ssa2*Δ pNBDsw, green: *ssa1*Δ
689 *ssa2*Δ pSBDsw, and dark green: *ssa1*Δ *ssa2*Δ pCTDsw. B) Heat sensitivity test of wildtype
690 (WT), and *ssa1*Δ *ssa2*Δ with the empty vector (pRS415), wild type Ssa1 and Ssa4 (*pSSA1*
691 and p*SSA4*), and each of the three chimeric versions of Ssa4 (p*NBDsw*, p*SBDsw* and
692 p*CTDsw*). The strains were serial diluted $1x10^{-1}$-$1x10^{-5}$ and plated on synthetic medium agar

693 plates for 3 days at the indicated temperatures. C) Fluorescent microscopy images of GFP-
694 Hsp104 in wild type cells carrying the empty vector (pRS415), wild type Ssa1 and Ssa4 (*pSSA1*
695 and p*SSA4*), and each of the three chimeric versions of Ssa4 (p*NBDsw*, p*SBDsw* and
696 p*CTDsw*), under exponential growth at 30 °C (control) and heat shock (42°C, 30 minutes). D)
697 Quantification of cells with foci from B. Columns represent the mean of 3 biological replicates,
698 *n* = 200-209. Dark grey: pRS415, white: pSSA1, light grey: pSSA4, light green: pNBDsw,
699 green: pSBDsw, and dark green: pCTDsw. Error bars: +/- S.D. E) Global alignment of Ssa1
700 and Ssa4. Conservation bar indicates the number of conserved physiochemical properties
701 between the residues where * = conserved residue, + = all properties conserved, 9 - 1 = almost
702 all to one property conserved, - = insertion/deletion/gap. Arrows (↓) mark residues previously
703 identified as important in Ssa1-Hsp104 interactions (30). Shaded boxes over residue codes
704 indicate domain demarcations; light grey: NBD, grey: SBD, dark grey: CTD

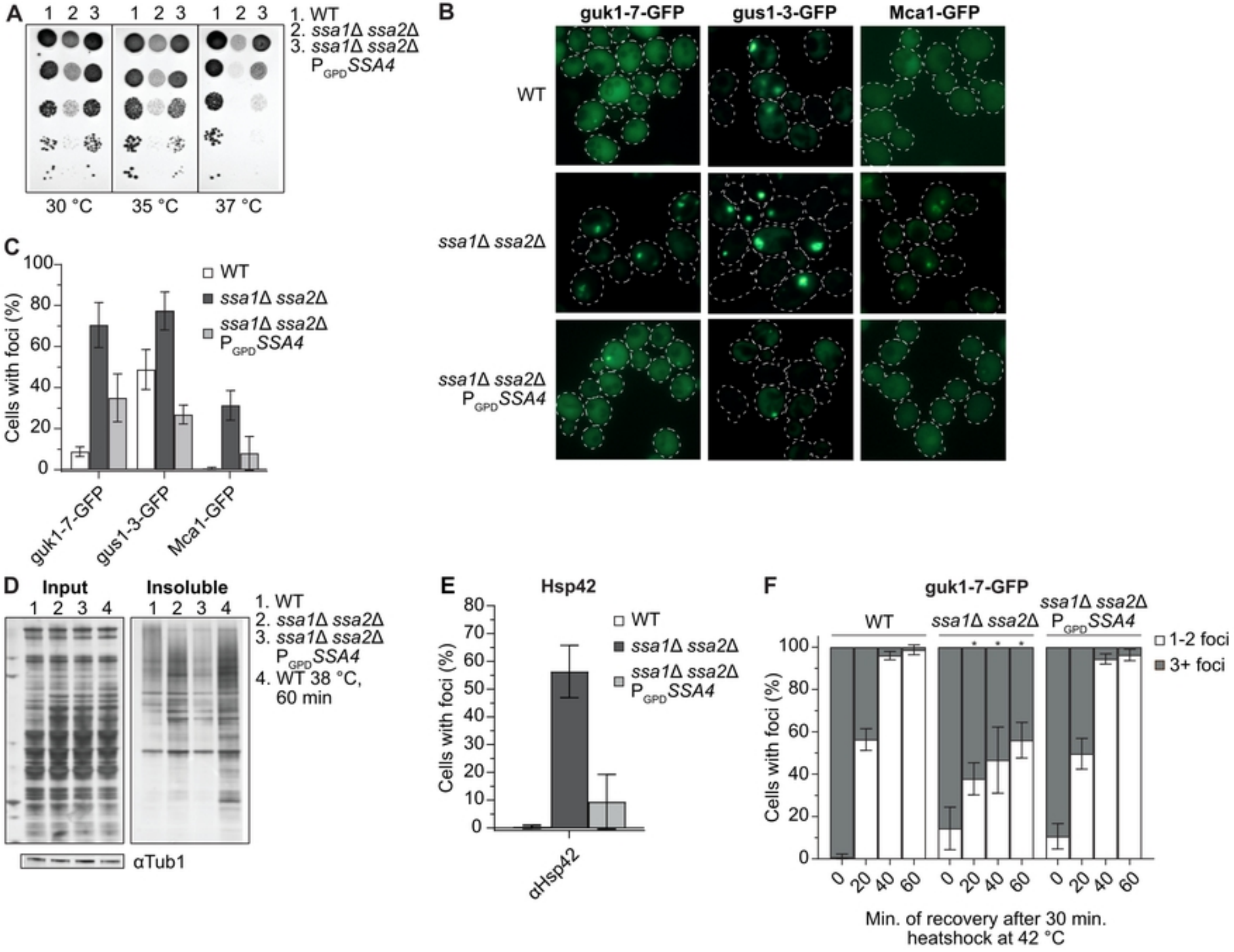
A
1 2 3 1 2 3 1 2 3
1. WT
2. ssa1Δ ssa2Δ
3. ssa1Δ ssa2Δ P GPD SSA4
30 °C
35 °C
37 °C
B
guk1-7-GFP
gus1-3-GFP
Mca1-GFP
WT
ssa1Δ ssa2Δ
ssa1Δ ssa2Δ P GPD SSA4
C
Cells with foci (%)
WT
ssa1Δ ssa2Δ
ssa1Δ ssa2Δ P GPD SSA4
guk1-7-GFP
gus1-3-GFP
Mca1-GFP
D
Input
Insoluble
1 2 3 4
1. WT
2. ssa1Δ ssa2Δ
3. ssa1Δ ssa2Δ P GPD SSA4
4. WT 38 °C, 60 min
αTub1
E
Hsp42
Cells with foci (%)
WT
ssa1Δ ssa2Δ
ssa1Δ ssa2Δ P GPD SSA4
αHsp42
F
guk1-7-GFP
WT
ssa1Δ ssa2Δ
ssa1Δ ssa2Δ P GPD SSA4
1-2 foci
3+ foci
Cells with foci (%)
0 20 40 60
Min. of recovery after 30 min. heatshock at 42 °C

Fig1

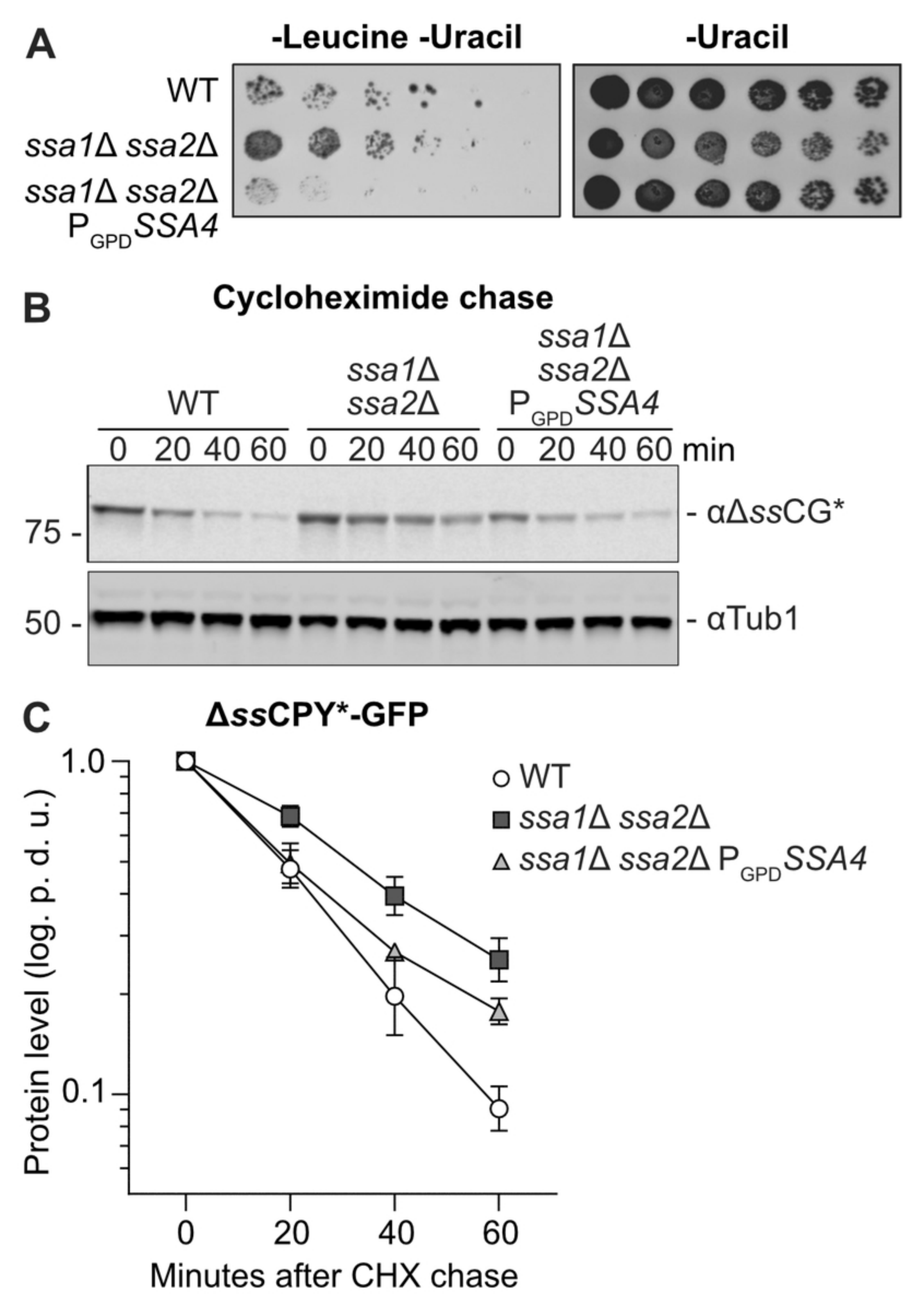
A
-Leucine -Uracil
-Uracil
WT
ssa1Δ ssa2Δ
ssa1Δ ssa2Δ
P GPD SSA4
B
Cycloheximide chase
WT
ssa1Δ
ssa2Δ
ssa1Δ
ssa2Δ
P GPD SSA4
0 20 40 60 0 20 40 60 0 20 40 60 min
75 -
- αΔssCG*
50 -
- αTub1
C
ΔssCPY*-GFP
1.0
0.1
Protein level (log. p. d. u.)
WT
ssa1Δ ssa2Δ
ssa1Δ ssa2Δ P GPD SSA4
0
20
40
60
Minutes after CHX chase

Fig2

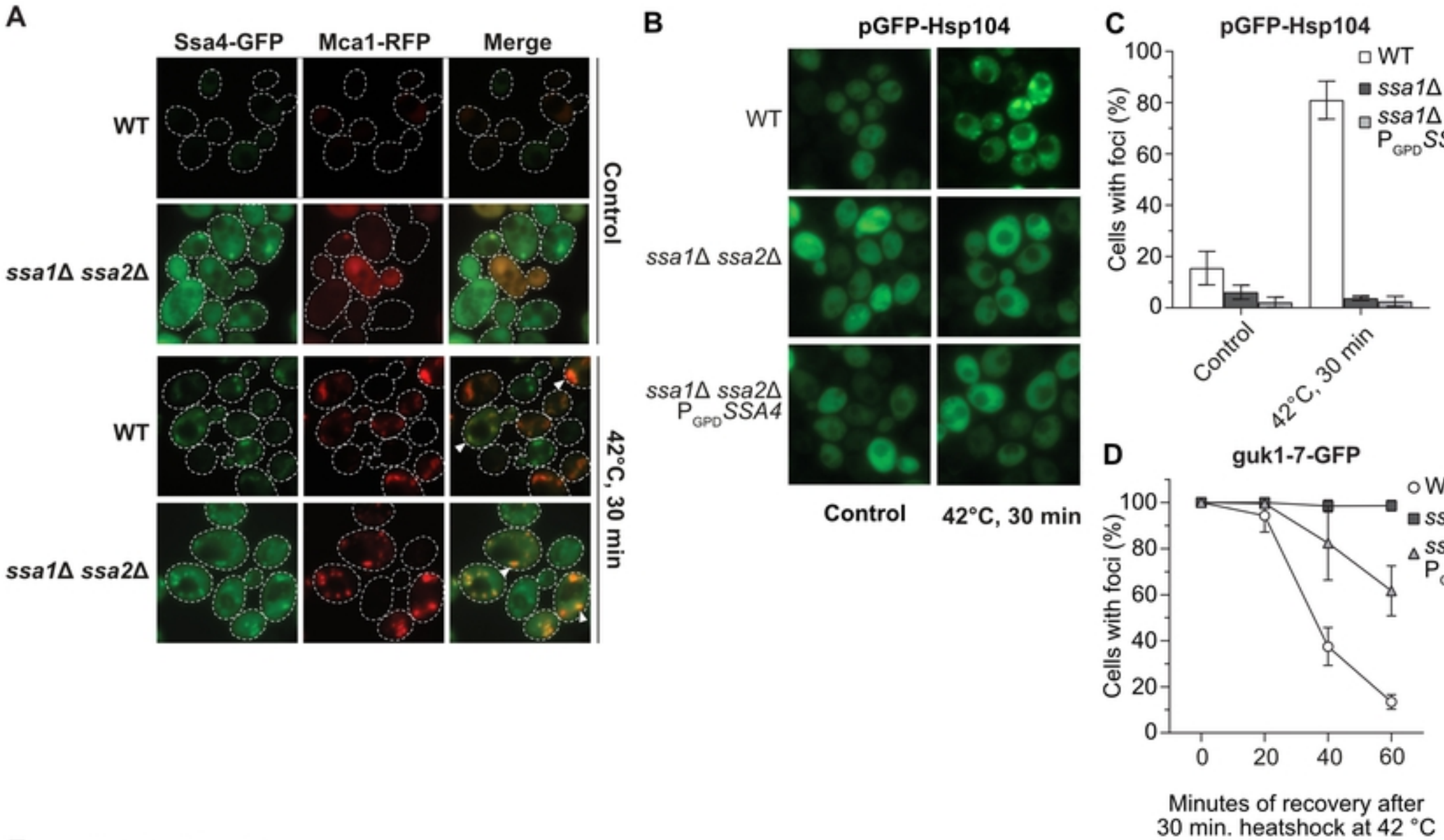
A
Ssa4-GFP
Mca1-RFP
Merge
WT
ssa1Δ ssa2Δ
Control
WT
ssa1Δ ssa2Δ
42°C, 30 min
B
pGFP-Hsp104
WT
ssa1Δ ssa2Δ
ssa1Δ ssa2Δ P GPD SSA4
Control
42°C, 30 min
C
pGFP-Hsp104
Cells with foci (%)
WT
ssa1Δ ssa2Δ
ssa1Δ ssa2Δ P GPD SSA4
Control
42°C, 30 min
D
guk1-7-GFP
Cells with foci (%)
WT
ssa1Δ ssa2Δ
ssa1Δ ssa2Δ P GPD SSA4
Minutes of recovery after 30 min. heatshock at 42 °C

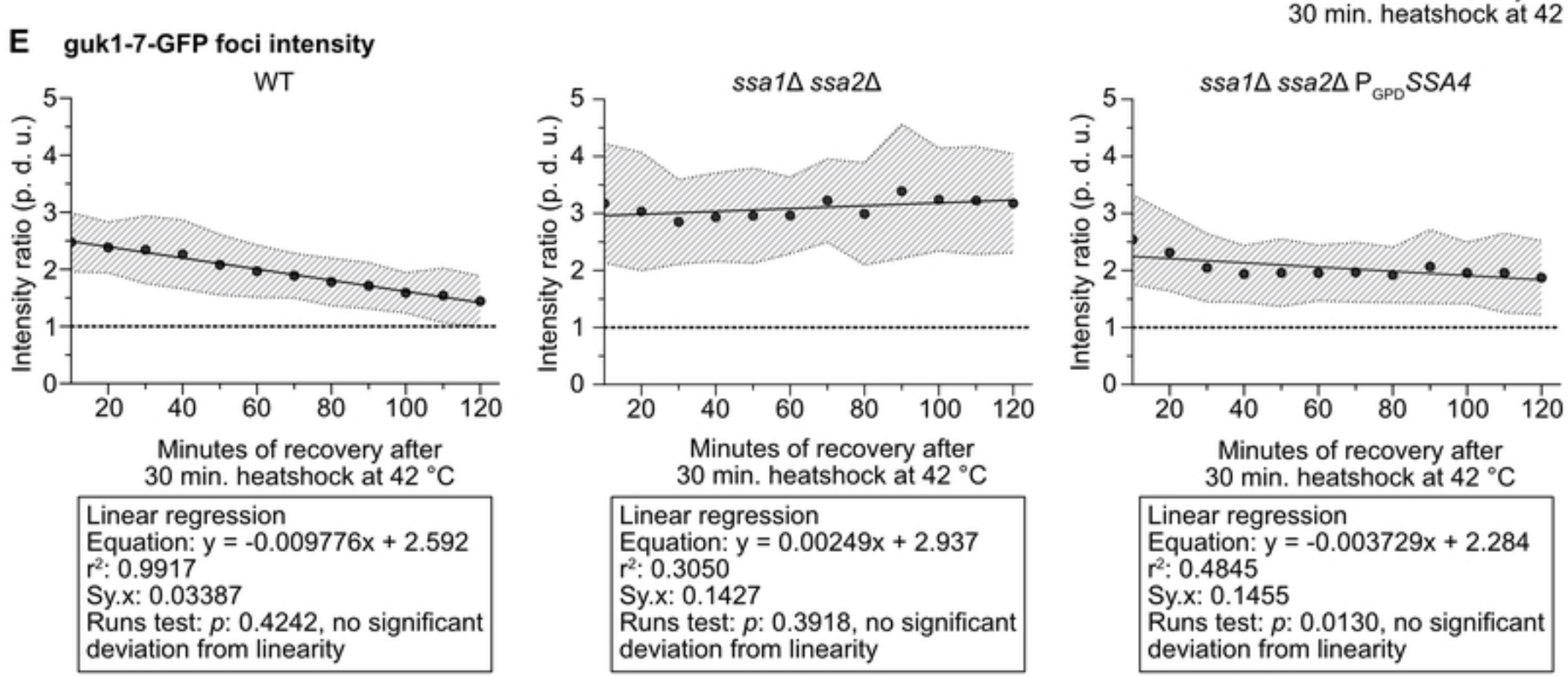
E guk1-7-GFP foci intensity
WT
ssa1Δ ssa2Δ
ssa1Δ ssa2Δ P GPD SSA4
Intensity ratio (p. d. u.)
Minutes of recovery after 30 min. heatshock at 42 °C
Linear regression
Equation: y = -0.009776x + 2.592
r²: 0.9917
Sy.x: 0.03387
Runs test: p: 0.4242, no significant deviation from linearity
Linear regression
Equation: y = 0.00249x + 2.937
r²: 0.3050
Sy.x: 0.1427
Runs test: p: 0.3918, no significant deviation from linearity
Linear regression
Equation: y = -0.003729x + 2.284
r²: 0.4845
Sy.x: 0.1455
Runs test: p: 0.0130, no significant deviation from linearity

Fig3

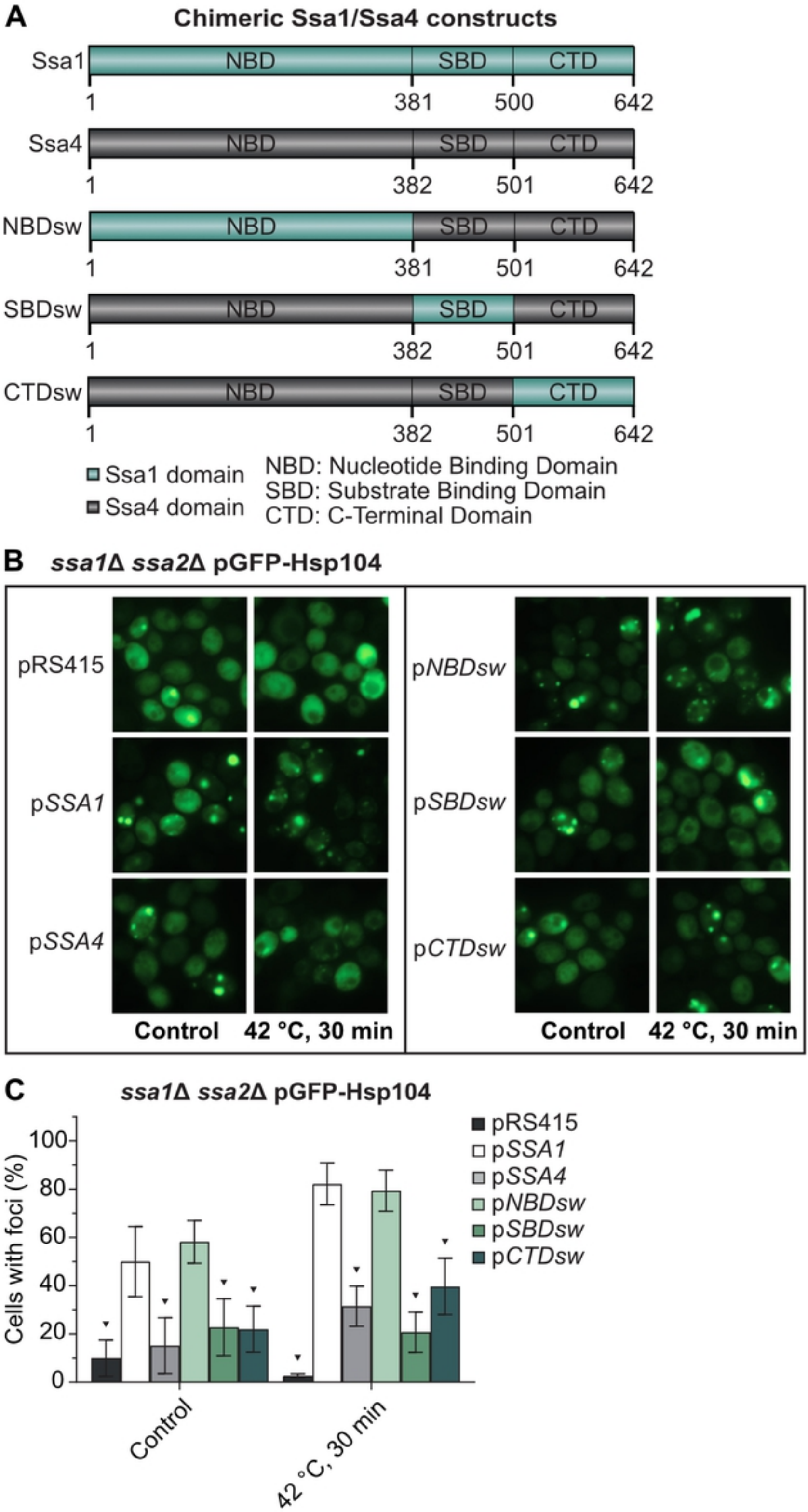
A
Chimeric Ssa1/Ssa4 constructs
Ssa1
NBD
SBD
CTD
1
381
500
642
Ssa4
NBD
SBD
CTD
1
382
501
642
NBDsw
NBD
SBD
CTD
1
381
501
642
SBDsw
NBD
SBD
CTD
1
382
501
642
CTDsw
NBD
SBD
CTD
1
382
501
642
Ssa1 domain
Ssa4 domain
NBD: Nucleotide Binding Domain
SBD: Substrate Binding Domain
CTD: C-Terminal Domain
B
ssa1Δ ssa2Δ pGFP-Hsp104
pRS415
pSSA1
pSSA4
pNBDsw
pSBDsw
pCTDsw
Control
42 °C, 30 min
Control
42 °C, 30 min
C
ssa1Δ ssa2Δ pGFP-Hsp104
Cells with foci (%)
100
80
60
40
20
0
pRS415
pSSA1
pSSA4
pNBDsw
pSBDsw
pCTDsw
Control
42 °C, 30 min

Fig4

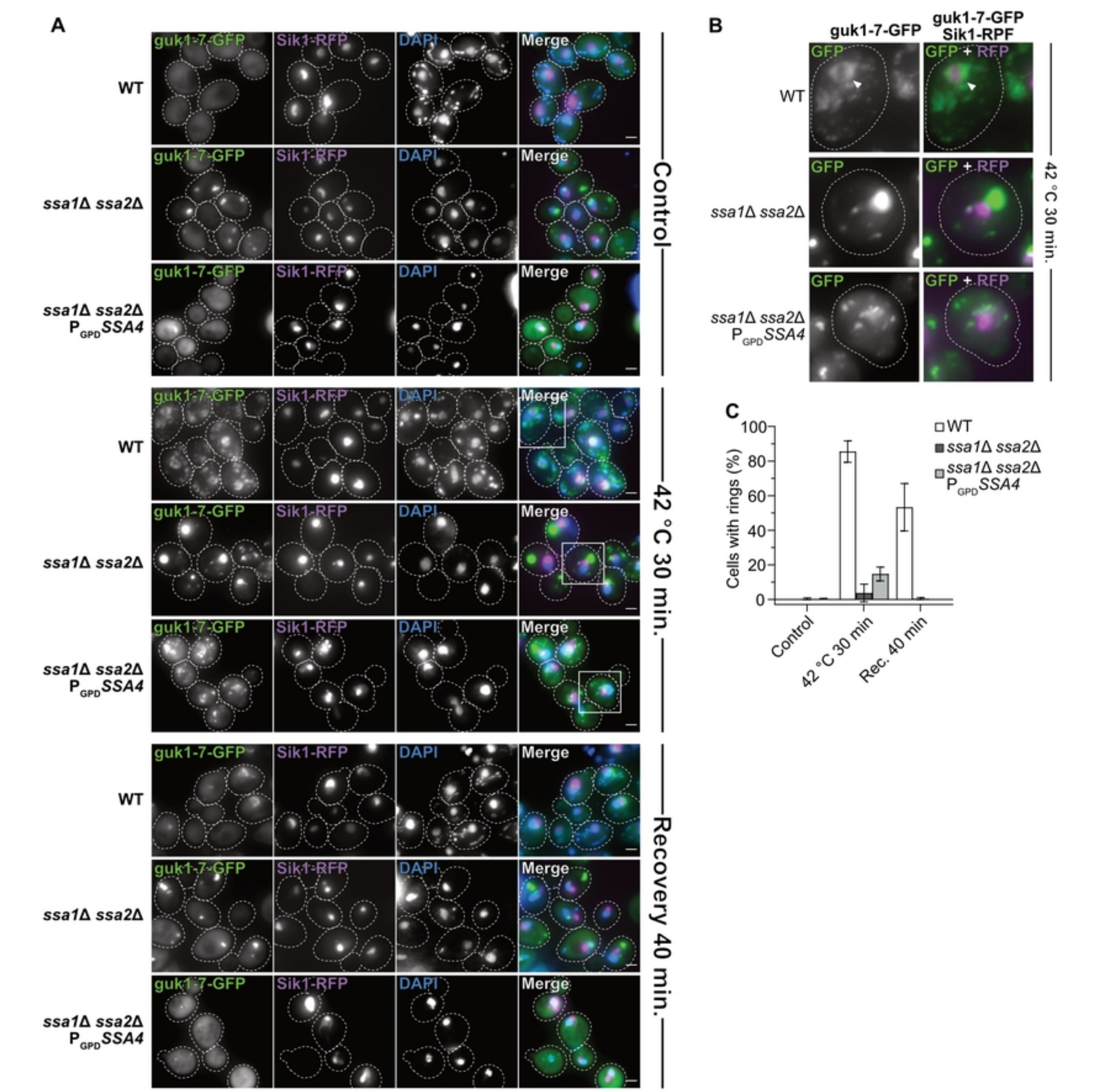
A
guk1-7-GFP
Sik1-RFP
DAPI
Merge
WT
ssa1Δ ssa2Δ
ssa1Δ ssa2Δ
P GPD SSA4
Control
42 °C 30 min.
Recovery 40 min.
B
guk1-7-GFP
guk1-7-GFP
Sik1-RPF
GFP
GFP + RFP
42 °C 30 min.
C
Cells with rings (%)
100
80
60
40
20
0
WT
ssa1Δ ssa2Δ
ssa1Δ ssa2Δ
P GPD SSA4
Control
42 °C 30 min
Rec. 40 min

Fig5

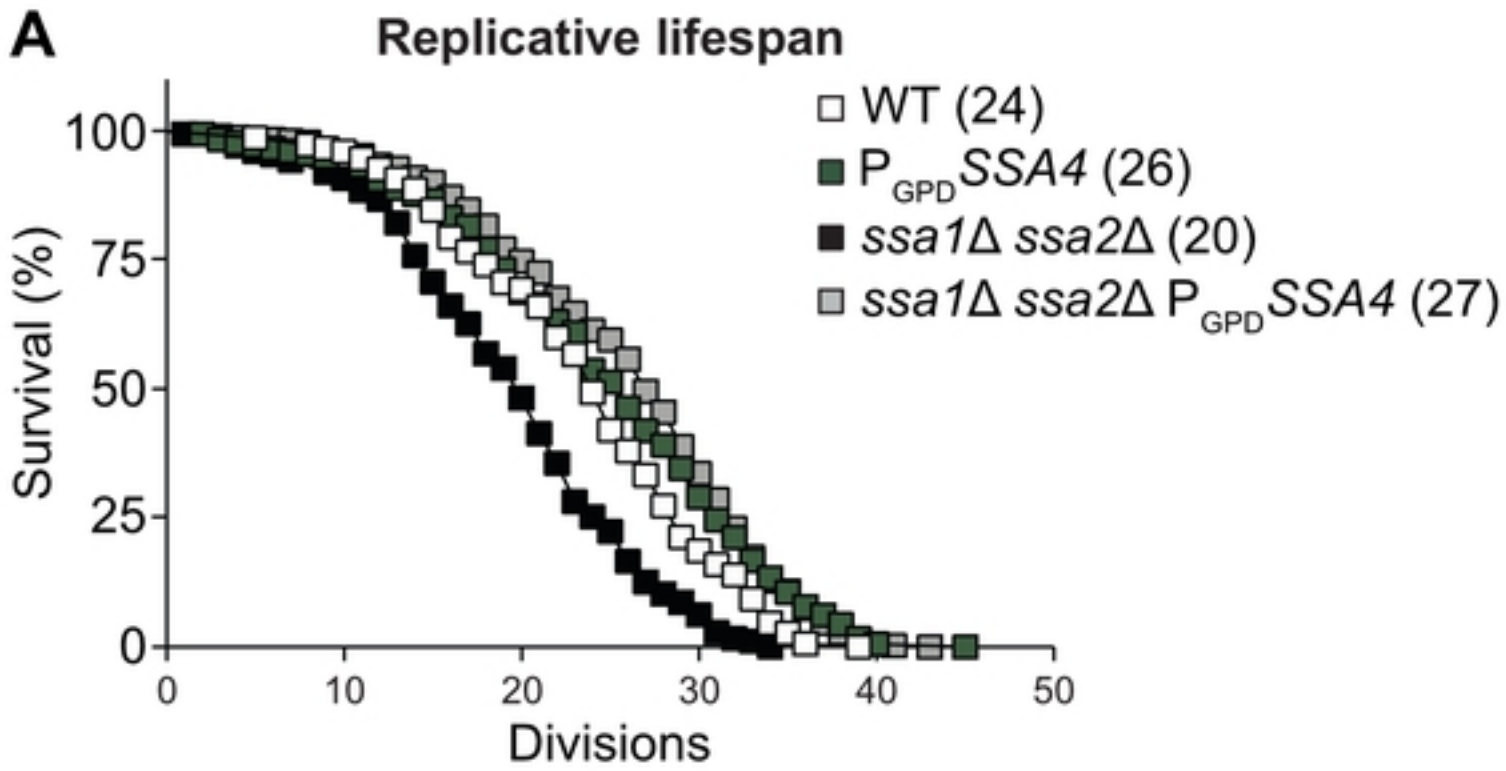
A
Replicative lifespan
WT (24)
P GPD SSA4 (26)
ssa1Δ ssa2Δ (20)
ssa1Δ ssa2Δ P GPD SSA4 (27)
Survival (%)
100
75
50
25
0
0
10
20
30
40
50
Divisions

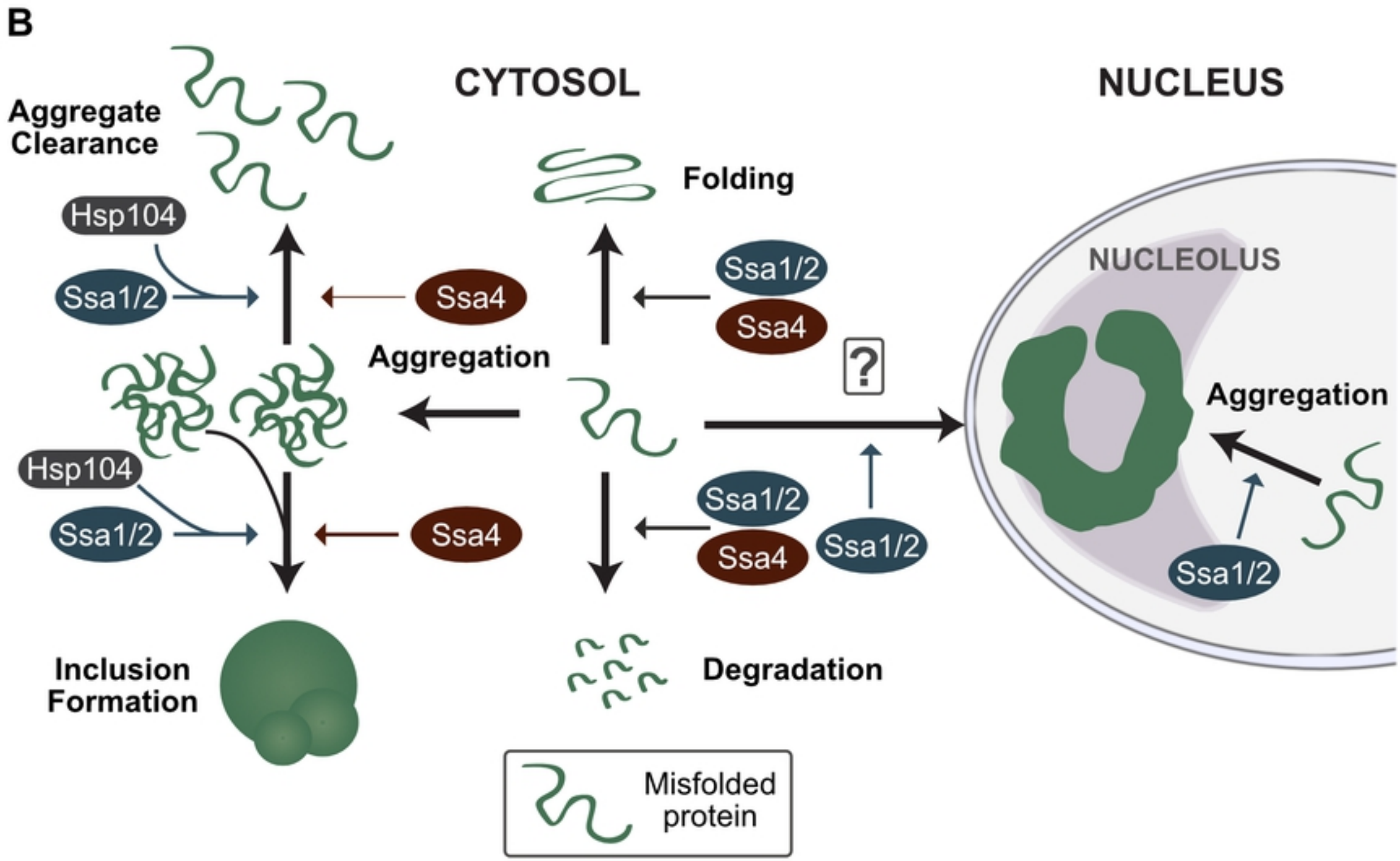
B
CYTOSOL
NUCLEUS
Aggregate Clearance
Hsp104
Ssa1/2
Ssa4
Aggregation
Folding
Ssa1/2
Ssa4
?
NUCLEOLUS
Aggregation
Hsp104
Ssa1/2
Ssa4
Ssa1/2
Ssa4
Ssa1/2
Ssa1/2
Inclusion Formation
Degradation
Misfolded protein

Fig6